# Improved Photocatalytic Activity of Pd-doped ZnO Nanoparticles Synthesized by Combustion Method

## Irine T. Ma and Rathika Ab\*

<sup>a</sup>Research Scholar (Reg.No: 19213092132011), Department of Physics, Muslim Arts College, Thiruvithancode, Kanyakumari, Tamilnadu, India.

b\*Department of Physics and Research Centre, Muslim Arts College, Thiruvithancode, Kanyakumari, Tamilnadu, India.

Affiliated to Manonmaniam Sundaranar University, Abishekapatti, Tirunelveli, Tamilnadu, India.

# **Abstract**

Herein, pure ZnO and Pd (3.0wt %) doped Zno nanoparticles was synthesized using simple chemical Combustion method. The incorporation of Pd with ZnO shows the excelled photocatalytic activity due to its high crystalline nanostructure. The X-ray diffraction spectrum endorsed that Pd-doped ZnO sintered at a temperature of 500 °C has Zincite-type natured material. The SEM analysis depicts the Pd-doped ZnO composite has a spherical sized particle range from 47nm and 70 nm respectively. From UV-visible absorption spectrum it is observed that synthesized zinc oxide and Pd doped ZnO composite has a band gap of 3.4 eV and 3.2 eV. In this context, Pd-doped ZnO act as an efficient UV light active photocatalyst results in the degradation of Mb dye within 45 min. Due to the high crystallinity of Pd- doped ZnO nanoparticle shows high photocatalytic activity than pure ZnO nanoparticles. Thus our findings emphasis that the Pd- doped ZnO nanoparticle would be the most proficient candidate for the removal of water contamination.

**Key words:** Combustion, photocatalytic activity, Pd-doped ZnO, Dye degradation.

## 1. INTRODUCTION

The textile and leather industry mainly depends on dyes owing to their colour giving properties. Thus it leads to the production of newly formed tons of commercial dyes

[1–4]. The industries that use dyes is textile industry may consume over than ten thousand tons of dyes worldwide per year [5]. It has been determined that the dye wastewater from textile industry results in the difficulty of complete attachment of the dye mixture onto a piece of fabric or textile [6]. Numerous hazardous chemicals such as organic resins, organic solvents hydrogen peroxide, formic acid, dispersing agents, soap, caustic soda, sulphuric acid, and hydrosulphate are included in dye wastewater. All these chemicals are known by its hazard and toxic effects towards the lives of humans and animals owing to their toxic nature [7, 8]. Lately, elimination of dye molecules from wastewater is a critical issue among the global environmental concern [9]. Various procedures of dye removal from wastewater have been proposed, each of them has its own advantage and disadvantages [10, 11].

In the view of fact, two significant factors are strongly governing the effectiveness of dye removal method namely time is the process of removal of dye and the production of secondary pollutants. Clearly, the effective way of dye removal from wastewater should be the elimination of large quantities of dyes molecules in short period of time without yielding a more secondary dangerous product. Investigators have involved three categories of dye removal processes from wastewater firstly the biological method, it is characterized by their low cost and ease of performance whereas it is unable to remove dyes effectively from wastewater [12]. Secondly the chemical method which uses the chemistry and its theories to be accomplished the degradation mechanism. Numerous mechanisms may be intricate in chemical methods such as electrochemical, advanced oxidation processes (AOPs), reduction, ozonation, and Fenton reaction; this method is characterized by the high rate beside generation of secondary hazardous by-products [13]. Thirdly the physical method is commonly used to achieved through mass transfer mechanism; it performed through numerous strategies such as flocculation, reverse osmosis, adsorption, ion exchange, irradiation, membrane filtration, coagulation and ultra filtration [14, 15]. Chemical dye removal is the most effective method among all aforementioned methods although of its disadvantages [16].

The elimination of dyes such as methylene blue (MB) from industrial wastewater before discharging the waste is of furthest importance due to their carcinogenic and mutagenic reaction of their structure. Organic dyes colorize other materials in water, making them visible and visually unpleasant [17]. Also, photosynthetic activities are hampered due to interference with sunlight penetration into water bodies, thus affecting fish and other aquatic organisms. Researchers stated that MB is not strongly hazardous but it has very injurious effects on living things [18]. So, the removal of MB from waste water is an essential task. About of the dyes are carcinogenic and mutagenic due to their molecular structure, functional group, and types such as benzidine and metals [19]. There are serious contrary effects with far-reaching consequences that are more attributed from the MB. The contact with eye can leads to enduring of blindness to human and animal's and also experiencing the short period of span or difficulty in breathing when inhaled. Likewise burning sensation when ingested through mouth, and also causes other adverse circumstances such as nausea, vomiting, profuse sweating, and mental confusion. Due to new increase in industrial

activities such as textile manufacturing, the use of dyes increases rapidly that significantly contaminated the water bodies. The recent statistical reports [20] emphasis that the rapid development of industrialization leads to the production of different types of dyes. They reported a global annual manufacture of these dyestuffs and intermediates estimated to be 7 × 108 kg. So, the elimination of dyes from wastewater received a great attention in recent years. Removal of these dyes from wastewater effluents is difficult as they possess a complex aromatic chemical structure that makes them highly visible and reduced photosynthetic activity in aquatic systems by reducing the light penetration [21]. On the other hand, photocatalytic degradation has been achieved for the methylene blue dye degradation using Pd/TiO2 nanocomposite. The prepared photocatalyst was characterized by several techniques. It was concluded that methylene blue dye has been successfully degraded by the synthesized nanocomposite photocatalyst under visible light irradiation within 3.5 h [22].

Photocatalytic degradation is one of the strongest AOPs, has been considered as one of the efficient way for the pollutant removal from wastewater in which the pollutants are degraded into non-toxic substances [23-27]. The choice of photocatalytic degradation is the most important technique in pollutant removal that would attribute to numerous factors such nontoxicity, great stability, no secondary pollution, lowprice, no need for severe conditions and efficient elimination of organic pollutants and dyes [28-32]. Many photocatalytic applications such as degradation of pollutants and contaminants might concern with utilization of numerous semiconductors [33-35]. In recent years, ZnO is being utilised as an alternate candidate to TiO2 due to their nontoxicity, sustainability, low cost, chemical and thermal stability, good catalytic efficiency and optoelectronic nature [36-39]. ZnO is also used in the various applications includes photovoltaic devices, water splitting and organic pollutants degradation.[40,41]. However, the most important problem of ZnO is the recombination rate of the photoexcited holes and electron that hinders their photocatalytic efficacy. Usually, the kinetics of the recombination rate is faster than that of the surface reduction-oxidation reactions, and this results in a reduction of the quantum efficiency of photocatalysis. Among the various semiconducting material, ZnO nanoparticles is one of the detailed studied semiconductor-type metal oxides with a band gap of ~ 3.37 eV[42,43]. It is known to be as one of the greatest photocatalysts for the degradation of environmental contaminants due to its high photocatalytic activity, relatively low cost, absence of toxicity, and excellent chemical stability under numerous conditions [44].

In adding to the photocatalytic water treatment, ZnO nanoparticles is widely used in a various applications includes solar cells [45], sensors [46], photoelectrochemical cells [47], antibacterial activity [48, 49], and photocatalysis [50, 51]. For all of the above-mentioned applications, nanoscopic ZnO are of best-suited in difference to the bulk or macroscopic ZnO. These ZnO nanoparticles not only provide high surface area but also offers appropriate bandgap for the separation of the exciton and thereby provides a feasible environment for enhanced photocatalytic activity [52]. Therefore, different methods have been stated for the synthesis of ZnO nanoparticles with a wide range of

morphologies (nanowires, nanorods, nanobelts, nanotubes and whiskers) using techniques such as ball-milling [53], combustion synthesis [54], sol-gel process [55], hydrothermal [56], spray pyrolysis [57], chemical vapor deposition [58], etc. [59] Most of these preparing procedures require sophisticated methods, instrumentation, expensive chemicals, and prolonged reaction time. Consequently, it is essential for the development of a facile and environmentally friendly method for the synthesis of ZnO nanoparticles (1-100 nm in size) with the highly active of photocatalytic and other applications. Different methods have been used to reduce the electron- hole recombination rate and these include the introduction of semiconductor oxides. carbonaceous materials and noble metals [60]. Noble metals nanoparticles such as Au, Ag, Pt and Pd have been reported to enhance the photocatalytic activity of ZnO [61-63]. In assessment with Pt and Au, Pd is cheaper and it has been employed in catalytic processes. Pd nanoparticles can act as collectors for the photoexcited electrons and this aid the charge transfer and transportation processes, thereby creating more active sites for the catalytic reaction [64]. The aim of this study is to synthesize of ZnO nanoparticles with different weight percentage of palladium leads to the effective photo generated charge carrier's for the degradation of environmental pollutants. The enhancement of photo catalytic activity of the composite was evaluated by the uv light radiation over the methylene blue

#### 2. EXPERIMENTAL PROCEDURE

#### 2.1. Materials

Zinc Nitrate ( $Zn(NO_3)_2$  6 $H_2O$ ), Glycine ( $C_2H_5NO_2$ ), Citric acid ( $C_6H_8O_7$ ), Palladium chloride (PdCl<sub>2</sub>), Methylthioninium chloride (Methylene blue -  $C_{16}H_{18}ClN_3S$ ) and Distilled water was used all over the experiment.

#### 2.2. Preparation of ZnO Nanoparticles

The Stoichiometric amount of oxidant(1): fuel(4) such as zinc nitrate: mixture of Glycine and Citric acid are taken in a 100 ml beaker. To that above solution about 30 ml of water is added and stirred until the solution became homogeneous mixture. The above mixture is boiled and evaporated in a hot plate stopped until it reaches foamy nature with evolution of pale yellow bubbles. Finally, combustion reaction occurred instantaneously leading to explosion reaction taking place within the beaker results the formation of ZnO nanoparticles. The obtained ZnO nanoparticles were calcined at 500 °C f or 4 hour.

### 2.3. Synthesis of palladium doped zinc oxide nanoparticles

Pd-doped ZnO composite were synthesized by simple chemical combustion method using precursor materials such as zinc nitrate (Zn(NO<sub>3</sub>)<sub>2</sub>·6H<sub>2</sub>O), glycine (C<sub>2</sub>H<sub>5</sub>NO<sub>2</sub>) and Citric acid (C<sub>6</sub> H<sub>8</sub> O<sub>7</sub>) and dopant as Zinc nitrate and Palladium chloride(3.0 wt%) acted as oxidant while glycine and citric acid as fuel during the course of the

reaction. The Stoichiometric amount of oxidant(1): fuel(4) such as zinc nitrate with palladium chloride(3.0 wt%): mixture of Glycine and Citric acid are taken in a 100 ml beaker and mixed thoroughly. To the above mixture 30 ml of water is added and stirred to form a homogeneous solution. The above mixture is boiled and evaporated in a hot plate stopped until it reaches foamy nature with evolution of brownish colour bubbles. Finally, combustion reaction occurred instantaneously leading to explosion reaction taking place within the beaker results the formation of Pd-doped ZnO nanoparticles. The obtained Pd-doped ZnO nanoparticles were calcined at 500 °C f or 4 hour.

## 2.4. Photocatalytic experiment

For the photocatalytic experiment , about 50 mL of methylene blue dye solution was taken in a100 ml beaker and 0.1 g Pd-doped ZnO was added with continuous stirred and kept in dark condition for 2 hr to reach the adsorption-desorption equilibrium. After 2 hr in dark the solutions were subjected to irradiation of UV lamp (Philips TUV 15 W/G15 T8(UV-C, $\lambda$ max=253.7nm)) with continuous stirring to carry out the photocatalytic experiment. Then the solution was taken every 5 minutes interval and centrifuged at 5000 rpm for 10 min. The aliquot solution analyzed under UV Visible spectrophotometer at absorbance 660nm corresponds to Methylene blue dye for 45 minutes to reach complete degradation.

#### 3. RESULTS AND DISCUSSION

## 3.1. XRD Analysis

Figure 1 shows the XRD spectra of (a) Pure ZnO, and (b) 3wt.% Pd doped ZnO. From fig 1(a) it obvious that prepared ZnO was in hexagonal wurtzite structure corresponds to the JCPDS no 65-3411[] assigned to the planes of (100), (002), (101), (102), (110), (103), (200), (112), (201), (004) and (202). The peak assigned from the diffracted pattern corresponds to hexagonal wurtzite structure of ZnO particle. Fig 1. (b) represents the diffracted peaks of Pd doped ZnO. There was no other diffracted peak of pd observed in the composite. It was similar to the pure ZnO diffracted peak but there was a significant decrease in the intensity of the diffracted peak due to the minimal doping of Pd in the composite. The absence of dopant peak in XRD confirmed that the prepared materials are highly pure but the crystallite size of the particles was increased. The results show that Pd - doped ZnO sample has a better crystallinity, higher intensity even after the addition of the small amount of Pd, but the peaks for Pd were not observed which are similar with the previously reported literature [65]. The crystalline size and lattice parameters are given in the table 1. The crystalline sizes of the ZnO and Pd doped ZnO were determined by means of X-ray line –broadening method using Debye–Scherrer's formula [66,67]

$$D = \frac{k\lambda}{\beta \cos \theta}$$

where  $\lambda$  is the wavelength of the X-ray (0. 1541 A°), the FWHM (full width at half maximum) of the more intense peak, and the diffraction angle, and D is the particle diameter size.

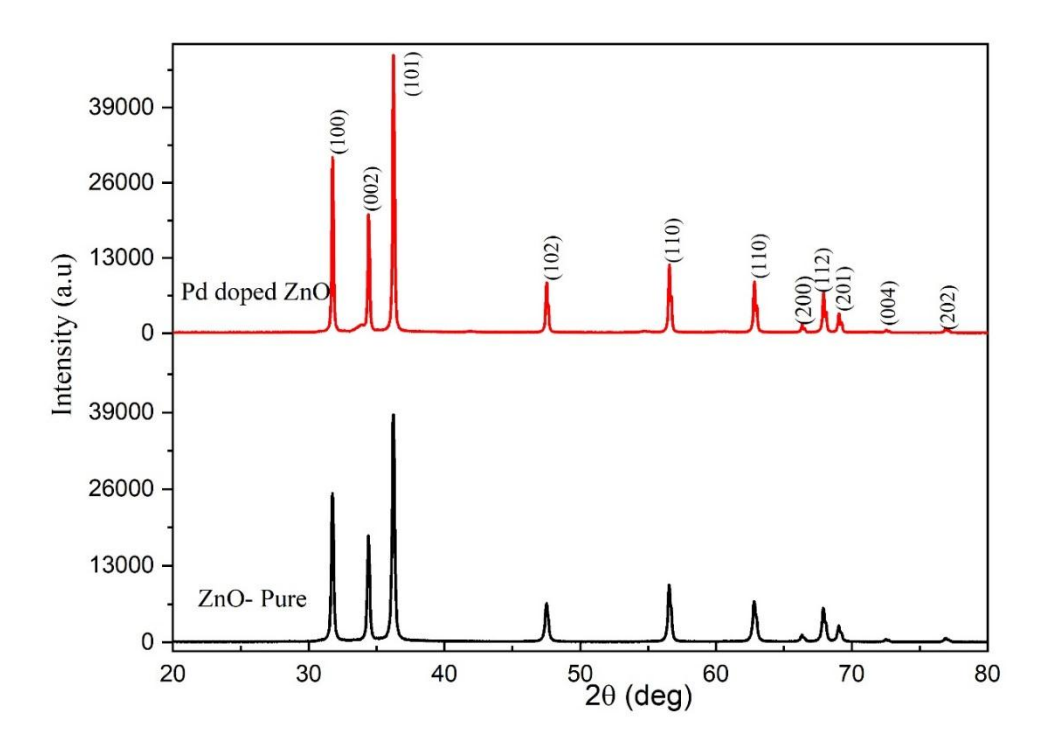


Figure 1. XRD Patterns of a) ZnO Pure and b) Pd Doped ZnO

**Table 1.** Displays the crystallite sizes and lattice parameters of pure ZnO and Pd doped ZnO.

Sample	Temperature	a = b(A)	c (Å)	Cell volume (ų)	D (nm)	Goodness of fitting
ZnO	700	3.2519	5.2098	47.712	47	1.79
	500					
Pd-ZnO		3.2906	5.3021	49.72	70	2.11

# 3.2. Thermogravimetric Analysis

Thermogravimetric analysis is used to determine thermal stability of the sample while increasing the temperature. The absorbed water content was determined from the

weight difference measured at 30°C -800° C for the pure ZnO and Pd doped ZnO. From Fig. 2(a-b) it is obvious that the temperature range between 30 -100° C represents the presence of absorbed water molecule or moisture observed from the composite []. The relative weight loss percentage of 7% and 3% corresponds to the pure ZnO and Pd doped ZnO. Then the second weight loss stage starts at 100°C -500°C, about 5% and 15% loss observed for ZnO and Pd doped ZnO at 500°C. The net weight loss 22% was observed beyond 700°C. From Fig.2 b, Palladium doped 3% sample a substantial net weight loss corresponding to 8% at 400°C is observed.

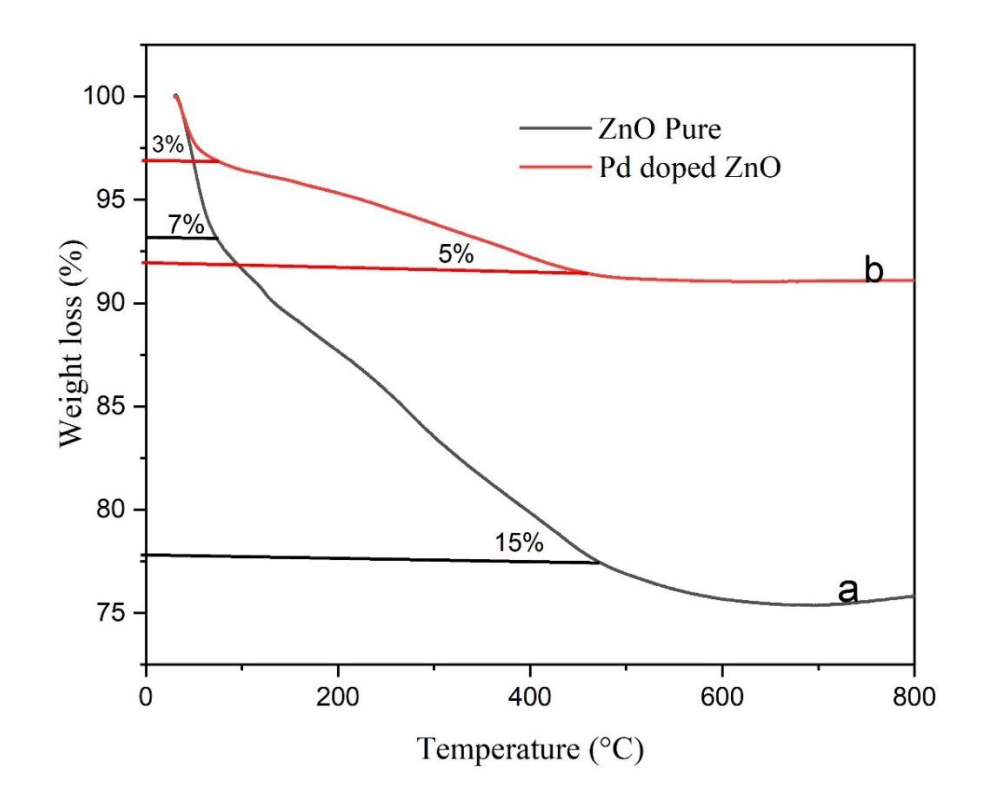


Figure 2. Thermogravimetric of ZnO Pure, Pd Doped ZnO

# 3.3. UV-Visible absorption Analysis

UV-Visible absorption spectroscopy is widely being used technique to examine the optical properties of nanosized particles. The absorption spectrum of ZnO and Pd doped ZnO composite is shown in Fig.3 The characteristic spectrum of fundamental absorption edge at 364 nm was observed for the pure ZnO. Pd doped ZnO nanocomposite shows the enhanced absorption than ZnO nanoparticle. The prepared ZnO and Pd doped ZnO showed strong absorption below 400 nm in near-UV spectral region, confirming the wide band of ZnO semiconductor material. This is due to the Pd doped into the nanocomposite which aided the separation and transportation of the photogenerated charge carriers [68]. Also, the surface plasmon resonance property of Pd played a key role in enhancing the light absorption [69].

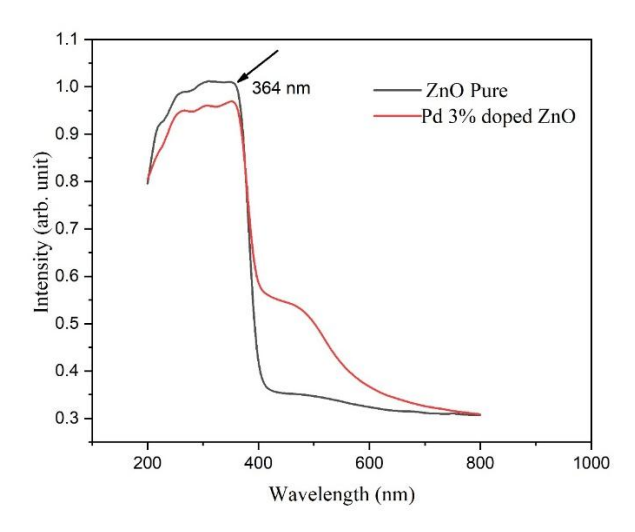


Figure 3. UV absorbance spectrum of ZnO Pure, Pd Doped ZnO

# 3.4. Band gap Analysis

The optical band-gap of the ZnO pure and Pd doped ZnO composite can be determined with a well-known Tauc's model by using Mott and Davis relation  $\alpha hv \sim (hv - \text{Eg})^{\frac{1}{2}}$  where Eg is energy band gap [70]. Following this relation, the band gap is attained by extrapolating the tangential line of  $(\alpha hv)^2$  to the photon energy axis. The direct bandgap energies can be estimated from a plot of  $(\alpha hv)^2$  versus the energy. From the Fig. 6, band gap for Pd doped ZnO nanoparticles are found to be 3.2 eV range and for pure samples 3.4 eV. The doping of palladium with ZnO nanoparticles leads to the reduction in band gap energy. It can be seen that the band gap of the ZnO nanoparticles decreased by adding palladium.

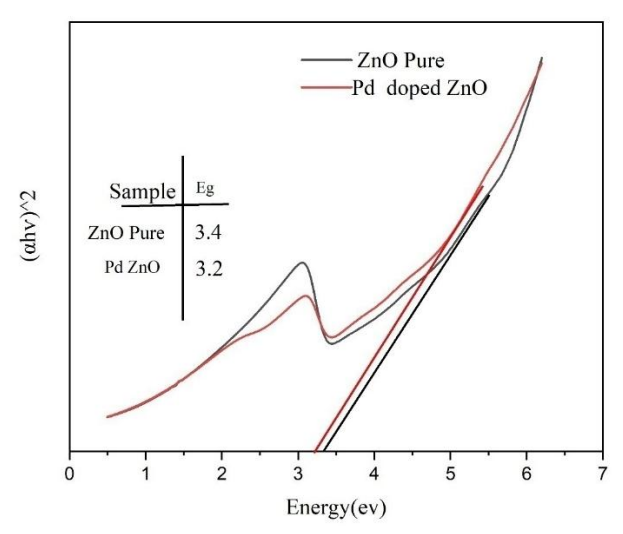


Figure 4. Band gap spectrum of ZnO Pure, Pd Doped ZnO

# 3.5. FTIR Analysis

The composition and quality of the material was investigated by the FTIR spectroscopy Figure 5. Shows bands at about 680 and 500 cm<sup>-1</sup> attributed to the formation of the stretching vibration of metal-oxygen (Zn–O) bonds. The characteristic peaks are given in the Table. 2. Typically, infrared spectra shows the characteristic bands of ZnO in the region from 900 cm<sup>-1</sup> up to 500 cm<sup>-1</sup> which can be used for qualitative characterization and confirmation of the shape of ZnO particles[71]. Pd doped ZnO composite, shows that there is a band at 3491 cm<sup>-1</sup> corresponding to the vibration mode of water OH group indicating the presence of small amount of water adsorbed on the ZnO nano crystal surface [72] which was correlated with TGA spectrum.

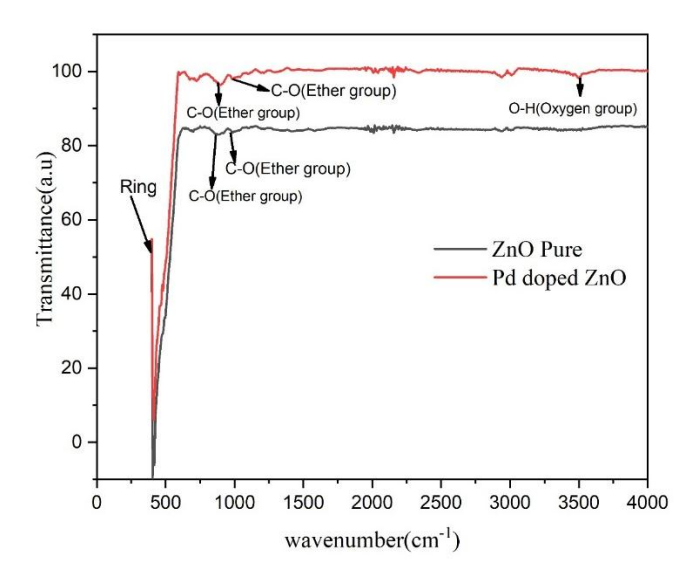


Figure 5. FTIR spectrum of ZnO Pure and Pd Doped ZnO Nanoparticles

**Table 2.** Characteristic peaks in FTIR spectrum of ZnO and Pd doped ZnO at 350° C

Sample	Peak values frequency cm <sup>-1</sup>	Bond	Functional group
	418.55	Ring	Meta
ZnO	983.70	C-O	Ether group
	879.54	C-O	Ether group
	412.77	Ring	Meta
D11 17 0	898.83	C-O	Ether group
Pd doped ZnO	1039.63	C-O	Ether group
	3491.16	О-Н	Oxygen group

# 3.6. SEM and EDX spectrum Analysis

Figure 6. a, c represents the surface morphology and the elemental composition of Pd doped ZnO. It depicts that spherical shaped particles were evenly distributed. The morphology showed rather than a dispersion of particles and palladium was also deposited over the surface of ZnO. In Fig. 3b the size distribution histogram of the Pd doped ZnO is shown. The size distribution was obtained by measuring the size of 100 randomly picked nanoparticles using the ImageJ software. From the histogram, it was found that the Pd-ZnO had an average size of about 73 nm. EDX analysis provided the elemental composition of the materials is shown in Fig. 6 c, which revealed that the spectrum confirms the presence of Zn; O elements are present in the composite material. The presence of palladium elemental peaks is also confirmed through EDX spectrum which leads to the enhancement of photocatalytic activity.

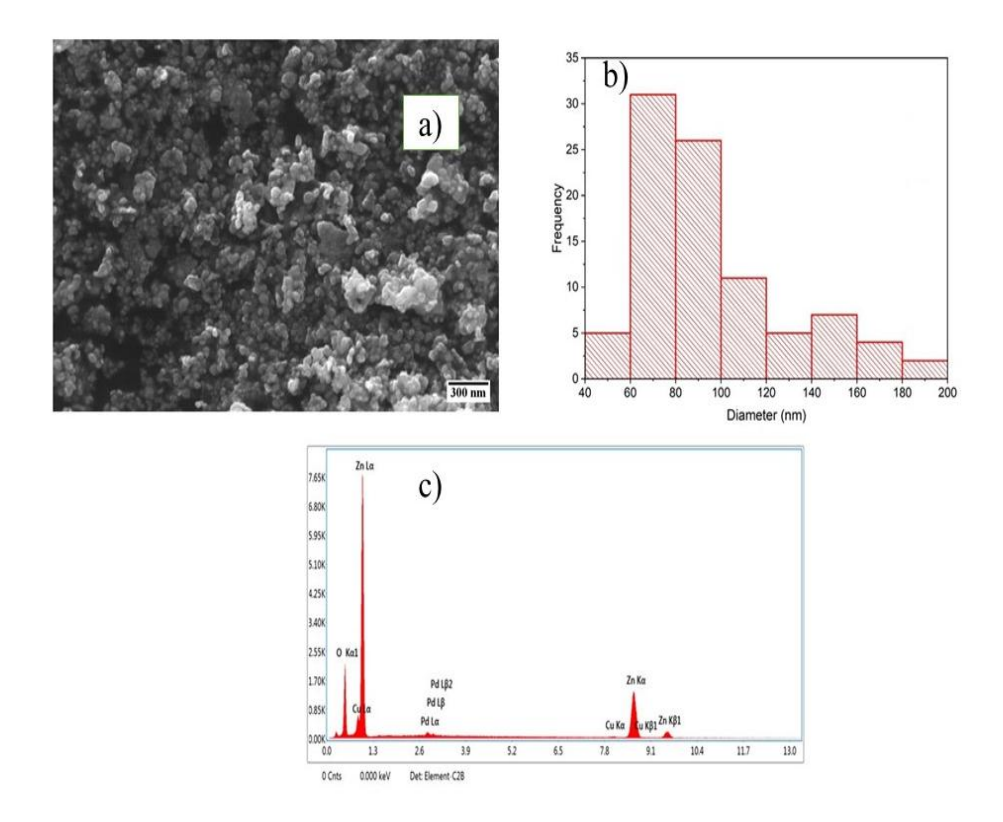


Figure 6. SEM image and EDAX spectrum of Pd Doped ZnO

## 3.7. Photocatalytic activity Analysis

After attaining equilibrium condition by exposing it in the dark for 120 min for both pure ZnO and Pd doped ZnO. It was observed that most dye molecules remained in the solution for pure ZnO while in comparison with Pd doped ZnO. Likewise, a larger amount of dye molecules were adsorbed on the surface of Pd doped ZnO composite. The photocatalytic activities of the samples were evaluated by the photocatalytic degradation of methylene blue (MB) dye under UV irradiation. The

UV-vis absorption spectra of MB at different irradiating intervals using the ZnO powders and Pd doped ZnO was evaluated. The intensities of the absorption peak situated at 660 nm decrease with the increase of the irradiation time, indicating that the concentration of MB in the solution is reduced gradually. The photocatalytic activity of different ZnO and Pd doped ZnO composite is shown in Fig.7. a,b Moreover, it was found that ZnO had little ability to mineralize MB under UV light irradiation. The samples prepared with Pd doped ZnO exhibit higher photocatalytic activity. After exposing with 45 min of light irradiation, the order of photocatalytic activities of Pd doped ZnO composite (3%) prepared weight percentage can be ordered as follows: Pd-ZnO(3 %) > ZnO.

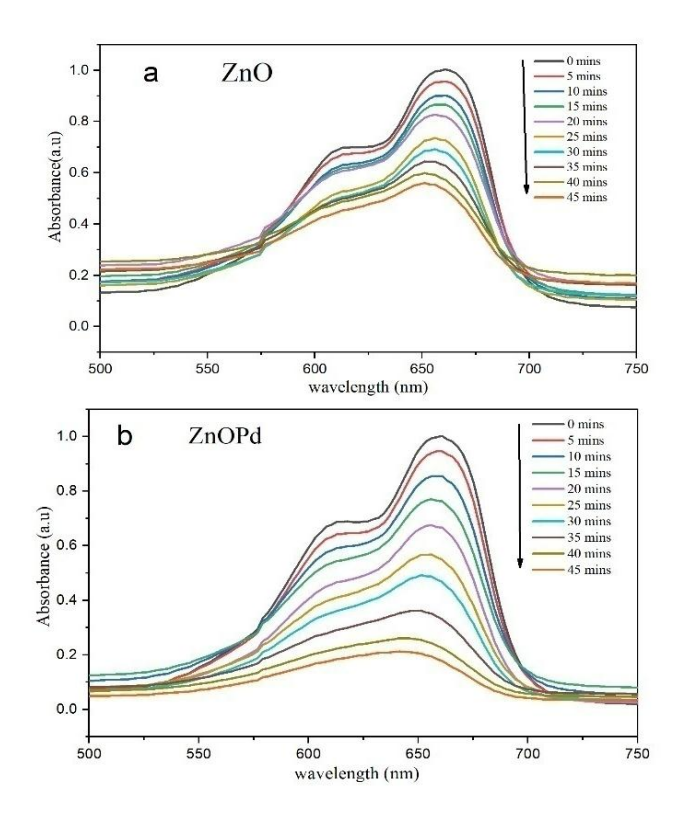
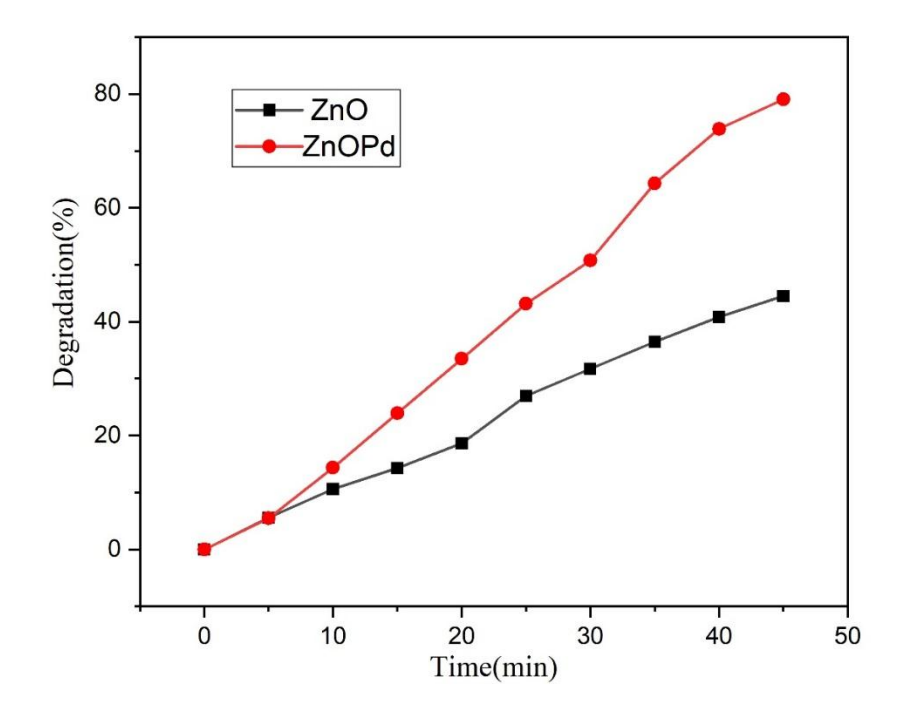


Figure 7. Photocatalytic activity ZnO Pure and Pd doped ZnO

## 3.8. Degradation percentage Analysis

The time-dependent percent degradation of methylene blue in DW by different ZnO and Pd-ZnO samples is shown in Fig. 8. The percentage of degradation was significantly increased for the Pd doped ZnO composite and nearly attained maximum degradation efficiency of 90 % under 45 minutes of UV light irradiation. On the other hand, pure ZnO comparatively has slower activity of 45% of MB dye decolorized after 45 min. The result emphasis that the photocatalytic activities of (ZnO-Pd) are

higher than that of pure ZnO. Because the palladium metal acts as electron sink, therefore it enhanced the electron-hole charge separation and reduced the charge recombination process. This process promotes the production of hydroxide radical and superoxide radical generation [73, 74]. These generated active radicals are act as effective degradation agents for the methylene blue dye molecules.



**Figure 8.** Degradation percentage of ZnO Pure and Pd doped ZnO

#### 4. CONCLUSION

Thus pure ZnO and ZnO-Pd nanocomposite materials have been successfully synthesized by a combustion technique and characterized by TGA, UV, XRD, EDX and SEM. The Pd-doped ZnO nanoparticles containing 3.0 wt % of Pd with a particle size of 70 nm composed of Zincite-type ZnO. The XRD pattern and EDX analysis confirmed the presence of crystalline nature and the elemental composition of Zn, O, Pd of the composite. The SEM analysis depicts the spherical sized particles of ZnO-Pd nanocomposite materials. The photocatalytic activity of composite was investigated by the degradation of Methylene blue under UV irradiation. Whereas, Pd doped ZnO has achieved a maximum degradation efficacy of 90% after 45 mins of UV light irradiation. It was significantly higher than the pure ZnO leads to the higher adsorption ability of light. The efficient removal of methylene blue is due to the generation of the higher concentration of hydroxyl radicals due to the presence of Pd. Therefore zinc oxide-palladium nanocomposite material exhibits excelled

photocatalytic activity due to the adverse effect of palladium that promotes the photo catalytic degradation of methylene blue. This paper gives a new insight for the development of some other composite material for the waste water management.

#### REFERENCES

- [1] Abdi, J., Vossoughi, M., Mahmoodi, N.M., Alemzadeh, I., 2017, "Synthesis of metal-Organic framework hybrid nanocomposites based on GO and CNT with high adsorption capacity for dye removal", Chem. Eng., 326, 1145–1158.
- [2] Crini, G., 2006, "Non-conventional low-cost adsorbents for dye removal: a review", Bioresour. Technol., 97, 1061–1085.
- [3] Gupta, V.K. & Suhas., 2009, "Application of low-cost adsorbents for dye removal—a review", Environmental Management, 90, 2313–2342.
- [4] Holkar, C.R, Jadhav, A.J, Pinjari, D.V, Mahamuni, N.M, Pandit, A.B., 2016, "A critical review on textile wastewater treatments: possible approaches", Environmental Management, 182, 351–366.
- [5] Rodríguez-Couto, S., Osma, J.F., Toca-Herrera, J.L., 2009, "Removal of synthetic dyes by an eco-friendly strategy", Eng. Life Sci., 9, 116–123.
- [6] Robinson, T., McMullan, G., Marchant, R., Nigam, P., 2001, "Remediation of dyes in textile effluent: a critical review on current treatment technologies with a proposed alternative", Bioresour. Technol., 77, 247–255.
- [7] Al-Alwani, M.A.M., Norasikin, A.L., Mohamad, A., Kadhum, A.A.H., Mukhlus, A., 2018, "Application of dyes extracted from Alternanthera dentata leaves and Musa acuminata bracts as natural sensitizers for dye-sensitized solar cells", Spectrochim. Acta Part A: Mol. Biomol., 192, 487–498.
- [8] Liu, L., Zhang, J., Tan, Y., Jiang, Y. Hu, M., Li, S., Zhai, Q., 2014, "Rapid decolorization of anthraquinone and triphenylmethane dye using chloroperoxidase: catalytic mechanism, analysis of products and degradation route", Chem. Eng. J., 244, 9–18.
- [9] Joshi, M., Bansal, R., Purwar, R., 2003, "Colour removal from textile effluents", Indian J. Fibre Text, 29, 239–259.
- [10] Forgacs, E., Cserháti, T., Oros, G., 2004, "Removal of synthetic dyes from wastewaters: a review", Environ. Int., 30, 953–971.
- [11] Manavi, N., Kazemi, A.S., Bonakdarpour, B., 2007, "The development of aerobic granules from conventional activated sludge under anaerobic-aerobic cycles and their adaptation for treatment of dyeing wastewater", Chem. Eng. J., 312, 375–384.
- [12] Pan, Y., Wang, Y., Zhou, A., Wang, A., Wu, Z., Lv, L., Li, X., Zhang, K., Zhu, T., 2017, "Removal of azo dye in an up-flow membrane-less bioelectrochemical system integrated with bio-contact oxidation reactor", Chem. Eng. J. 326, 454–461.

- [13] Dos Santos, A.B., Cervantes, F.J., Lier, J.B., 2007, "Review paper on current technologies for decolourisation of textile wastewaters: perspectives for anaerobic biotechnology", Bioresour. Technol., 98, 2369–2385.
- [14] Hashem, F.S., Amin, M.S., 2016, "Adsorption of methylene blue by activated carbon derived from various fruit peels", Desalin. Water Treat., 57, 22573–22584.
- [15] El-Gamal, S.M.A., Amin, M.S., Ahmed, M.A., 2015, "Removal of methyl orange and bromophenol blue dyes from aqueous solution using Sorel's cement nanoparticles", J. Environ. Chem. Eng., 3, 1702–1712.
- [16] Wang, J., Qin, J., Lin, L., Zhu, J., Zhang, Y., Liu, J., Bruggen, B.V., 2017, "Enzymatic construction of antibacterial ultrathin membranes for dyes removal", Chem. Eng. J., 323, 56–63.
- [17] El-Khaiary, M. I., 2007, "Kinetics and mechanism of adsorption of methylene blue from aqueous solution by nitric-acid treated water-hyacinth", Journal of Hazardous Materials, 147, 28–36.
- [18] Ghosh., D., Bhattacharyya, K. G., 2002, "Adsorption of methylene blue on kaolinite", Applied Clay Science, 20, 295–300.
- [19] Lorenc-Grabowska, E., Gryglewicz, G., 2007, "Adsorption characteristics of Congo Red on coal-based mesoporous activated carbon", Dyes and Pigments, 74, 34–40.
- [20] Dogan, M., Abak, H., Alkan, M., 2009, "Adsorption of methylene blue onto hazelnut shell: kinetics, mechanism and activation parameters", Journal of Hazardous Materials, 164, 172–181.
- [21] Gullickson, N. D., Scamehornand, J. F., Harwell, J. H., 1989. "LiquidCoacervate Extraction-Surfactant Based Separation Processes, Marcel Dekker", New York, NY, USA.
- [22] Abdelaal, M.Y., Mohamed, R.M., 2013, "Novel Pd/TiO<sub>2</sub> nanocomposite prepared by modified sol–gel method for photocatalytic degradation of methylene blue dye under visible light irradiation". J. Alloys Compd., 576, 201–207.
- [23] Liang, S., Wen, L., Liu, G., Zhu, S., Yuan, R., Wu, L., 2013, "Comparative study of photocatalytic activities of Ca2Nb2O7 nanopolyhedra and TiO2: degradations of benzene and methyl orange", Catal. Today, 201, 175–181.
- [24] Sobahi, T.R., Amin, M.S., Mohamed, R.M., 2017, "Photocatalytic degradation of methylene blue dye by F doped Co3O4 nanowires", Desalin. Water Treat., 74, 346–353.
- [25] Aljahdali, M.S., Amin, M.S., Mohamed, R.M., 2018, "Gd-cobalt selenite as an efficient nanocomposite for aniline synthesis from photocatalytic reduction of nitrobenzene", Mater. Res. Bull. 99, 161–167.

- [26] Sobahi, T.R., Amin, M.S., Mohamed, R.M., 2018, "Enlargement of photocatalytic efficiency of BaSnO3 by indium doping for thiophene degradation, Appl. Nanosci., 8, 557–563.
- [27] Baoum, A.A., Amin, M.S., Mohamed, R.M., 2018, "Decoration of SnO<sub>2</sub> nanosheets by AgI nanoparticles driven visible light for norfloxacin degradation", Appl. Nanosci., 8, 2093–2102.
- [28] Kou, J., Lu, C., Wang, J., Chen, Y., Xu, Z., Varma, R.S., 2017, "Selectivity enhancement in heterogeneous photocatalytic transformations", Chem. Rev., 117, 1445–1514.
- [29] Khaki, M.R.D., Shafeeyan, M.S., Raman, A.A.A., Daud, W.M.A.W., 2017, "Application of doped photocatalysts for organic pollutant degradation a review", J. Environ. Manag. 198, 78–94.
- [30] Chen, F., Ho, P., Ran, R., Chen, W., Si, Z., Wu, X., Weng, D., Huang, Z., Lee, C., 2017, "Synergistic effect of CeO2 modified TiO2 photocatalyst on the enhancement of visible light photocatalytic performance", J. Alloy. Comp., 714, 560–566.
- [31] Gómez-Pastora, J., Dominguez, S., Bringas, E., Rivero, M.J., Ortiz, I., Dionysiou, D.D., 2017, "Review and perspectives on the use of magnetic nanophotocatalysts (MNPCs) in water treatment", Chem. Eng. J., 310, 407–427.
- [32] Fan, Y., Han, D., Song, Z., Sun, Z., Dong, X., Niu, L., 2018, "Regulations of silver halide nanostructure and composites on photocatalysis", Adv. Comp. Hybrid Mater., 2, 269–299.
- [33] Wang, X., Liu, X., Yuan, H., Liu, H., Liu, C., Li, T., Yan, C., Yan, X., Shen, C., Guo, Z., 2018, "Noncovalently functionalized graphene strengthened poly(vinyl alcohol)", Mater. Des., 139, 372–379.
- [34] Lou, X., Lin, C., Luo, Q., Zhao, J., Wang, B., Li, J., Shao, Q., Guo, X., Wang, N., Guo, Z., 2017, "Crystal structure modification enhanced FeNb11O29 anodes for lithium-ion batteries", Chem. Electro. Chem., 4, 3171–3180.
- [35] Sun, Z., Zhang, L., Dang, F., Liu, Y., Fei, Z., Shao, Q., Lin, H., Guo, J., Xiang, L., Yerra, N., Guo, Z., 2017, "Experimental and simulation-based understanding of morphology controlled barium titanate nanoparticles under co-adsorption of surfactants", Cryst Eng Comm., 19, 3288–3298.
- [36] Becker, J., Raghupathi, K. R., St. Pierre, J., Zhao, D., Koodali, R. T., 2011, "Tuning of the crystallite and particle sizes of ZnO nanocrystalline materials in solvothermal synthesis and their photocatalytic activity for dye degradation", J. Phys. Chem. C, 115(28), 13844–13850.
- [37] Chen, X., He, Y., Zhang, Q., Li, L., Hu, D., 2010, "Fabrication of sandwich-structured ZnO/reduced graphite oxide composite and its photocatalytic properties", J. Mater. Sci., 45(4), 953–960.

- [38] Sun, F., Qiao, X., Tan, F., Wang, W., Qiu, X., 2012, "One-step microwave synthesis of Ag/ZnO nanocomposites with enhanced photocatalytic performance, J. Mater. Sci., 1–7.
- [39] Zhang, L., Du, L., Yu, X., Tan, S., Cai, X., Yang, P., Gu, Y., Mai, W., 2014, "Signi □ cantly enhanced photocatalytic activities and charge separation mechanism of Pd-decorated ZnO− graphene oxide Nanocomposites", ACS Appl. Mater. Interfaces, 6(5), 3623–3629.
- [40] Balachandran, S., Prakash, N., Swaminathan, M., 2016, "Heteroarchitectured Ag–Bi2O3–ZnO as a bifunctional nanomaterial", RSC Adv., 6(24), 20247–20257.
- [41] Umukoro, E. H., Peleyeju, M. G., Ngila, J. C., Arotiba, O. A., 2016, "Photocatalytic degradation of acid blue 74 in water using Ag– Ag2O–Zno nanostuctures anchored on graphene oxide, Solid State Sci., 51, 66–73.
- [42] Djurišić, A.B., Leung, Y.H., Ng, A.M.C., 2014, "Strategies for improving the efficiency of semiconductor metal oxide photocatalysis, Materials Horizons, 1, 400–410.
- [43] Król, A., Pomastowski, P., Rafińska, K., Railean-Plugaru, V., Buszewski, B., 2017, "Zinc oxide nanoparticles: synthesis, antiseptic activity and toxicity mechanism", Adv. Colloid Interf. Sci., 249, 37–52.
- [44] Kaur, J., Bansal, S., Singhal, S., 2013, "Photocatalytic degradation of methyl orange using ZnO nanopowders synthesized via thermal decomposition of oxalate precursor method", Phys. B Condens. Matter, 416, 33–38.
- [45] Hu, G., Guo, W., Yu, R., Yang, X., Zhou, R., Pan, C., Wang, Z.L., 2016, "Enhanced performances of flexible ZnO/perovskite solar cells by piezo-phototronic effect, Nano Energy, 23, 27–33.
- [46] Zhang, Y., Liu, C., Gong, F., Jiu, B., Li, F., 2017, "Large scale synthesis of hexagonal simonkolleit nanosheets for ZnO gas sensors with enhanced performances, Mater. Lett., 186, 7–11.
- [47] Barreca, D., Carraro, G., Gasparotto, A., Maccato, C., Altantzis, T., Sada, C., Bals, S., 2017, "Vapor phase fabrication of nanoheterostructures based on ZnO for photoelectrochemical water splitting, Adv. Mater. Interfaces, 4, 1700161.
- [48] Lu, Z., Gao, J., He, Q., Wu, J., Liang, D., Yang, H., Chen, R., 2017, "Enhanced antibacterial and wound healing activities of microporous chitosan-Ag/ZnO composite dressing", Carbohydr. Polym., 156, 460–469.
- [49] Mao, C., Xiang, Y., Liu, X., Cui, Z., Yang, X., Yeung, K.W.K., Wu, S., 2017, "Photo-inspired antibacterial activity and wound healing acceleration by hydrogel embedded with Ag/Ag@ AgCl/ZnO nanostructures", ACS Nano, 11, 9010–9021.
- [50] Wahab, R., Hwang, I.H., Kim, Y.S., Shin, H.S., 2011, "Photocatalytic activity of zinc oxide micro-flowers synthesized via solution method", Chem. Eng. J., 168, 359–366.

- [51] Abdullah, A.M., O'Shea, K.E., 2019, "TiO2 photocatalytic degradation of the flame retardant tris (2-chloroethyl) phosphate (TCEP) in aqueous solution: a detailed kinetic and mechanistic study", J. Photochem. Photobiol., A Chem., 377, 130–137.
- [52] Ullah, R., Dutta, J., 2008, "Photocatalytic degradation of organic dyes with manganese doped ZnO nanoparticles", J. Hazard. Mater., 156, 194–200.
- [53] Chen, D., Ai, S., Liang, Z., Wei, F., 2016, "Preparation and photocatalytic properties of zinc oxide nanoparticles by microwave-assisted ball milling", Ceram. Int., 42, 3692–3696.
- [54] Lin, C.S., Hwang, C.C., Lee, W.H., Tong, W.Y., 2007, "Preparation of zinc oxide (ZnO) powders with different types of morphology by a combustion synthesis method", Mater. Sci. Eng. B, 140, 31–37.
- [55] Azam, A., Ahmed, F., Arshi, N., Chaman, M., Naqvi, A.H., 2010, "Formation and characterization of ZnO nanopowder synthesized by sol–gel method", J. Alloys Compd., 496, 399–402.
- [56] Yogamalar, N.R., Bose, A.C., 2011, "Tuning the aspect ratio of hydrothermally grown ZnO by choice of precursor", J. Solid State Chem., 184, 12–20.
- [57] Joseph, B., Gopchandran, K.G., Manoj, P.K., Koshy, P., Vaidyan, V.K., 1999, "Optical and electrical properties of zinc oxide films prepared by spray pyrolysis", Bull. Mater. Sci., 22, 921–926.
- [58] Kim, S.W., Kotani, T., Ueda, M., Fujita, S., Fujita, S., 2003, "Selective formation of ZnO nanodots on nanopatterned substrates by metalorganic chemical vapor deposition", Appl. Phys. Lett., 83, 3593–3595.
- [59] Mirzaei, H., Darroudi, M., 2017, "Zinc oxide nanoparticles: biological synthesis and biomedical applications", Ceram. Int., 43, 907–914.
- [60] Wang, W. W., Zhu Y. J., Yang, L. X., 2007, "ZnO–SnO2 hollow spheres and hierarchical nanosheets: hydrothermal preparation, formation mechanism, and photocatalytic properties", Adv. Funct. Mater., 17(1), 59–64.
- [61] Gu, H., Yang, Y., Tian J., Shi, G., 2013, "Photochemical synthesis of noble metal (Ag, Pd, Au, Pt) on graphene/ZnO multihybrid nanoarchitectures as electrocatalysis for H2O2 reduction", ACS Appl. Mater. Interfaces, 5(14), 6762–6768.
- [62] Ma, S., Xue, J., Zhou Y., Zhang, Z., 2014, "Photochemical synthesis of ZnO/Ag2O heterostructures with enhanced ultraviolet and visible photocatalytic activity", J. Mater. Chem. A, 2(20), 7272–7280.
- [63] Wang, Y., Wang, Q., Zhan, X., Wang, F., Safdar M., He, J., 2013, "Visible light driven type II heterostructures and their enhanced photocatalysis properties: a review", Nanoscale, 5(18), 8326–8339.

- [64] Shi, W., Yan, Y., Yan, X., 2013, "Microwave-assisted synthesis of nano-scale BiVO4 photocatalysts and their excellent visiblelight-driven photocatalytic activity for the degradation of cipro □ oxacin", Chem. Eng. J., 215, 740–746.
- [65] Zhang, L., Du, L., Yu, X., Tan, S., Cai, X., Yang, P., Gu Y., Mai, W., 2014, "Significantly enhanced photocatalytic activities and charge separation mechanism of Pd-decorated ZnO– graphene oxide Nanocomposites", ACS Appl. Mater. Interfaces, 6, 3623–3629
- [66] Zhang, Y., Wang, Q., Xu, J., Ma, S., 2012, "Synthesis of Pd/ZnO nanocomposites with high photocatalytic performance by a solvothermal method", Applied surface science, 258, 10104–10109.
- [67] Kashif, M., Ali, M.E., Syed, M., Usman Ali., Hashim, U., 2013, "Sol–gel synthesis of Pd doped ZnO nanorods for room temperature hydrogen sensing applications", Ceramics International, 39, 6461-6466.
- [68] Hao, L., Gao, W., Liu, Y., Liu, Y., Han, Z., Xue, Q., 2016, "Zhu, J., Self-powered broadband, high-detectivity and ultrafast photodetectors based on Pd-MoS 2/Si heterojunctions", Phys. Chem. Chem. Phys., 18, 1131-1139.
- [69] Zuppella, P., Pasqualotto, E., Zuccon, S., Gerlin, F., Corso, A.J., Scaramuzza, M., De Toni, A., Paccagnella, A., Pelizzo, M.G., 2015, "Palladium on plastic substrates for plasmonic devices", Sensors, 15, 1138-1147.
- [70] Tauc, J., Grigorovici, R., Vancu, A., 1966, "The optical properties and electronic structure of amorphous germanium", The Optical Properties of Solids, 15, 627-637.
- [71] Umukoro, E.H., Peleyeju, M.G., Ngila, J.C., Arotiba, O.A., 2016, "Photocatalytic degradation of acid blue 74 in water using Age Ag 2 OeZno nanostuctures anchored on graphene oxide", Solid State Science, 51, 66-73.
- [72] Anas, S., Rahul, S., Babitha, K.B., Mangalaraja, R.V., Ananthakumar, S., 2015, "Microwave accelerated synthesis of zinc oxide nanoplates and their enhanced photocatalytic activity under UV and solar illuminations", Applied Surface Science, 355, 98-103.
- [73] Chang, Y, Xu J, Zhang, Y, Ma, S, Xin L, Zhu, L Xu, C, 2009, "Optical properties and photocatalytic performances of Pd modified ZnO samples", Physical Chemical: C, 113, 18761–18767.
- [74] Zhang, y., Wang, Q., Xu, J., Ma, S., 2012, "Synthesis of Pd/ZnO nanocomposites with high photocatalytic performance by a solvothermal method", Applied Surface Science, 258, 10104–10109.